

Estimating Scour Depth Around Bridge Piles Using Ssiim Software and Comparing its Results with Physical Model Results

Ebrahim Jafari, H. Hassunizadeh, Ehsan Zaredehdasht, Maryam Kiurani

Islamic Azad University_ Shoushtar Campus

Abstract: Estimating maximum scour depth is normally required in order to determine the depth of a bridge piles. The present paper uses SSIIM Software which considers flow and sediment equations in a three dimensional manner. The software models floe field around circular bridge pile by resolving Navier-Stokes three-dimensional equations and k-ε method, and by temporary solution of flow field and continuity equations variations of bottom levels around bridge pile was determined. In order to verify the results of the simulated model were compared with those of laboratory experiments. The results indicates that the model can be used with high accuracy to simulate scour and estimating scour depth around bridge piles.

Key words: scour, bridge pile, flow field, SSIIM software, local scour.

INTRODUCTION

Estimating scour depths around hydraulic structures including bridge piles is treated as a critical issue that, when considered, helps engineers reduce errors in designing hydraulic works with respect to geometry, location, depth in the bed as necessary control depths, hence developing reliable and economic designs. Different researches made efforts to develop an approach to be capable of determining maximum scour around bridge piles. However, due to its complexities of this issue and its governing equation and the variety of effective parameters on scour development, no inclusive method has been yet proposed for this purpose. This has made researchers to turn to experimental methods and the results of such experiments have long been used in form of experimental and semi-experimental equations.

Setting up experimental models, however, is costly, time-consuming and the results cannot be easily generalized to “actual conditions”. Therefore, the necessity of developing numerical models to turn governing equations of flow field and sediment to simpler and solvable equations by discontinuing governing equations and a application of simplifying assumptions is felt more than ever. One of the approaches to simulate three-dimensional flow field and sediment is SSIIM software which can model most of the hydraulic phenomena including scour around bridge piles with high accuracy. The advantage of this software is the three-dimensional solution to flow and sediment equations that results in reduced inaccuracies in estimating maximum scour depths. The following section briefly describes SSIIM model used to determine flow field and sediment around a simulated circular bridge pile and the results are compared with the available experimental data.

1. Governing Equations of Flow Field:

The governing equations of flow field are Navier-Stokes equations that by considering turbulence effects finally lead to Reynolds equations. These equations can be written for incompressible fluids with constant density as follows[15]:

$$\frac{\partial u_i}{\partial t} + U_j \frac{\partial U_i}{\partial x_j} = \frac{I}{P} \frac{\partial}{\partial x_j} (-P \delta_{ij} - \overline{p u_i u_j}) \quad (1)$$

where the first term on left indicates time variations while the adjacent the shows movement. Also, the first term on right is pressure term and the second one is Reynolds stress that requires a turbulence model to meet. These equations are solved using finite discontinuing volume method. The correction pressure algorithm is used in SIMPIE algorithm as default while SSIIM software can use this algorithm, too (Olsen, 2003).

2. k-ε Turbulence Model:

The software used by default k-ε turbulence model to model Reynolds stresses as follows:

$$\frac{\partial k}{\partial t} + U_j \frac{\partial k}{\partial x_j} = \frac{\partial}{\partial x_j} \left[\frac{U_T}{\sigma_k} \frac{\partial k}{\partial x_j} \right] + P_k - \varepsilon \tag{2}$$

PK model is obtained s follows:

$$P_k = u_T \frac{\partial u_j}{\partial x_i} \left[\frac{\partial U_j}{\partial x_i} + \frac{\partial U_i}{\partial x_j} \right] \tag{3}$$

By determining K, ε is modeled as follows:

$$\frac{\partial \varepsilon}{\partial t} + U_j \frac{\partial \varepsilon}{\partial x_j} = \frac{\partial}{\partial x_j} \left[\frac{u_T}{\sigma_k} \frac{\partial \varepsilon}{\partial x_j} \right] + C_{\varepsilon 1} \frac{\varepsilon}{k} P_k - C_{\varepsilon 2} \frac{\varepsilon^2}{k} \tag{4}$$

In above models, the value of C is constant and is not changed by the user (Olsen, 1999). Also, the model can use other turbulence models including k-ε with some RNG extensions, isotropic constant turbulence viscosity model, local k-ε based on wind shear stress, turbulence viscosity-shear stress ×0.11 (Keefer, 1971), local k-ε based on water velocity and non-isotropic constant turbulence viscosity models (Olsen, 2003).

3. Calculation of Water Surface Profile:

Water surface profile is determined by extrapolation of pressure into internal cells. A reference level in a real cell downstream is given where water surface is prevented from changing. The pressure in this cell (Pref) is selected as reference pressure and a pressure difference is calculated for each cell by deducing reference pressure. This pressure differences provide the displacement for each cell through equation below:

$$h_{ij} = \frac{1}{\rho g} (p_{ij} - p_{ref}) \tag{5}$$

Vertical movement is used only for water surface cells and is proportionate to vertical [surface] layers distribution such that cell sizes vertically to water depth is always a constant value.

4. Sediment Flow Calculations:

The governing equation over sediment field is as follows:

$$\frac{dz}{dt} + \frac{1}{1 - n_p} \frac{dq_b}{dx} = 0 \tag{6}$$

where qb is sediment load in river width unit (m³/Sec/m) and np is porosity of sediment particles. Sediments transferred include suspended load and bed load. The amount of suspended load is calculated by transfer-diffusion equation for sediment density c as follows (Olsen, 2003)

$$\frac{\partial c}{\partial t} + U_j \frac{\partial c}{\partial x_j} + w \frac{\partial c}{\partial z} = \frac{\partial}{\partial x_j} \left(r_T \frac{\partial c}{\partial x_j} \right) \tag{7}$$

where

W: average speed of sediment particle fall

r: diffusion factor

r=uT/sc

Sc: Schmidt number which equals 1.0 by default

Bed load (qb) is calculated by default using Van Rjin formula as follows:

$$\frac{q_b}{D_{50}^{1.5} \sqrt{\frac{(P_s - P_w)}{P_w}}} = 0.053 \frac{\left[\frac{t - t_c}{t_c} \right]}{D_{50}^{0.3} \left[\frac{(P_s - P_w)g}{P_w u^2} \right]^{0.1}} \quad (8)$$

5. Description of Ssim Model:

The present paper used SSII model (Olsen, 2007) for gridding and solving flow and scour equations. This model solves Navier-Stokes flow equations in three dimensions using finite volume discontinuity method. For discontinuing, a volume control and power method, which is a first order upstream method, was used. For algorithms in time, an implicit method was used. SIMPLE method was used to obtain pressure values in all cells except those near water surface to calculate vortex viscosity k-ε was used. For surface cells, flow continuity equations were used to calculate water surface movement. Water surface position was determined by extrapolation of calculated pressure of cells adjacent to surface. This method uses a point with fixed water surface downstream and Equation along water surface to determine water surface position. Vertical variations of water surface was applied to the upper grid line and lower lines moved according to relative distance from water surface. All gradients of variables were taken zero at water surface except k whose value was taken as zero. In addition, symmetrical boundary conditions were applied on outflow boundaries and flow velocities were determined at the inflow boundaries. Velocity distribution was horizontally uniform and vertically algorithmic. Flow speeds at inflow and outflow boundaries were so determined that as water surface varied, the flux would remain constant. In order to determine the speed near walls, Shlichting Rules (1969) were used. Sediment transport was calculated for bed load and suspended load. Sediment transport-diffusion was equation solved to obtain sediment density. The diffusion constant was obtained equal to that of vortex viscosity by turbulence model. After solving flow equation, the bed shear stress was calculated and used to determine by Van Rijn equation the sediment density for nearest cell to bed (Van Rijn, 1987). Sediment transport-diffusion equation was not solved for cells adjacent to cells while bed variations were determined for sediment load by solving mass survival equation. One of the important physical processes in studying scour is sediment transport. The critical shear stress reduction for sediment inception on sloping bed was obtained by equations suggested by Brooks (Van Rijn, 1987).

6. Simulation of Flow Field and Sediment near Bridge Pile Using Ssim Model:

The grid used for this model was a grid with different surface ratios. in the middle of grid, 1*1cm and in the rest of channel 5*1 cm cells were used. Seven layers at 0, 10, 20,30,50,70 and 100% of water depths were defined. Higher density of layers was in lower part of grid mainly due to more variations near bed. The cross section is shown in Fig. (1) and (2).

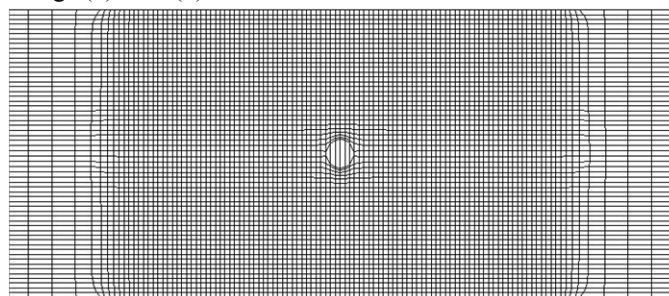


Fig. 1: The grid used for this model.

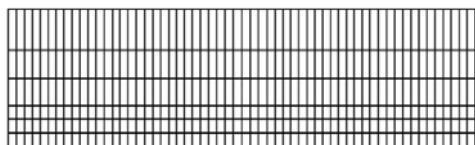


Fig. 2: The grid used for this model.

7. Model Sensitivity to Sediment Load Equations:

SSIIM software allows the user to select the intended sediment load formulae by F10 command in control file. The software uses Van Rjin, 1987 formulae by default. However, other formula developed by other researchers are allowed to be used by the user. As seen from Table (1), quatitive results obtained from using Yang, Shen and Hung equations are slightly inaccurate while the shape of scour hole by using Van Rjin, 1987 equation is more realistic from quality point of view. Hence, the use of default formulae is suggested to be used in SSIIM.

Table 1: Model Sensitivity to Sediment Load Equations.

Error (%)	scour depth	Pundit
34.40	23.52	Ackers / White
66.80	29.19	Engelund/Hansen
0.30	17.55	Yang
0.62	17.60	Shen / Hung
78.28	31.19	Einstein

8. Time Step:

The selection of the proper time step is quit important in model calibration stage. Generally, the following experimental equation is recommended for this purpose where b is channel width in cm, h is flow depth in cm, d is bridge diameter inn cm and t is time step in second. The obtained tie step is 4 seconds:

$$\Delta t = 1/67 \times 10^{-1} \frac{bd}{h}$$

9. Comparing Scour Depths by Numerical and Experimental Models in X and Y Directions:

Fig. (3),(4) compares scour depths around X direction. The numerical model underestimates scour depths by 10 to 20% in front and back of bridge pile than experimental results. The studies shows that in ... area, the measured scour depth is less than that of experimental results. Fig. (5),(6) compares scour depths along Y direction indicating an agreement between numerical and experimental results along X direction is as good as those along Y direction. Also, it is observed that the scour hole slope in front and back of bridge pile in both cases is hc/D=0.5 and hc/D=2.5, respectively, which is almost similar to that of experimental results.

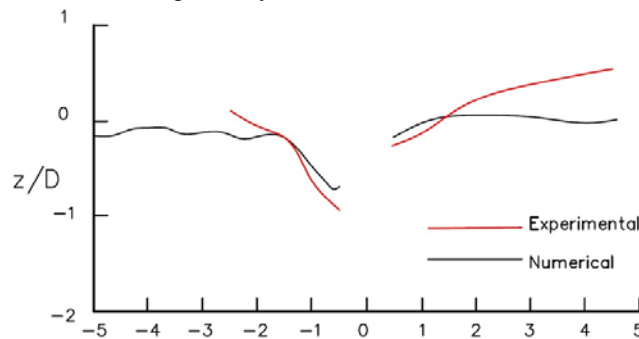


Fig. 3: Scour depth distribution along x-axis. (For $h_c/D=0.5$).

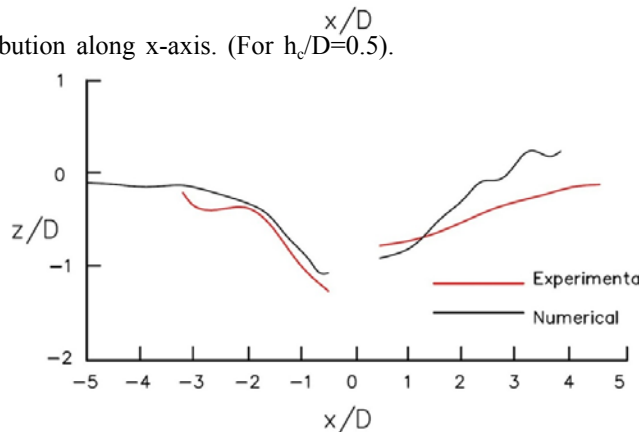


Fig. 4: Scour depth distribution along x-axis. (For $h_c/D=2.5$).

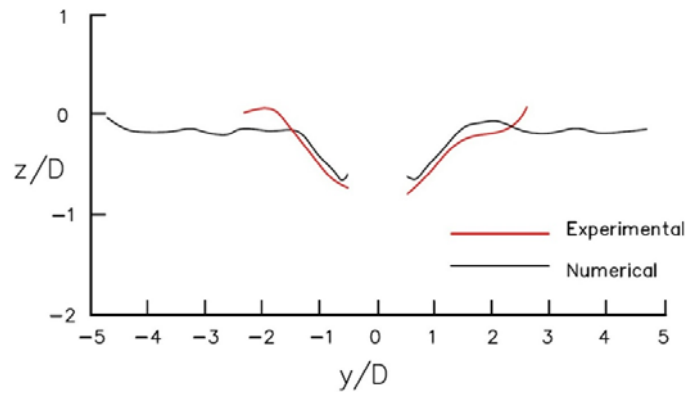


Fig. 5: Scour depth distribution along y-axis. (For $h_c/D=0.5$).

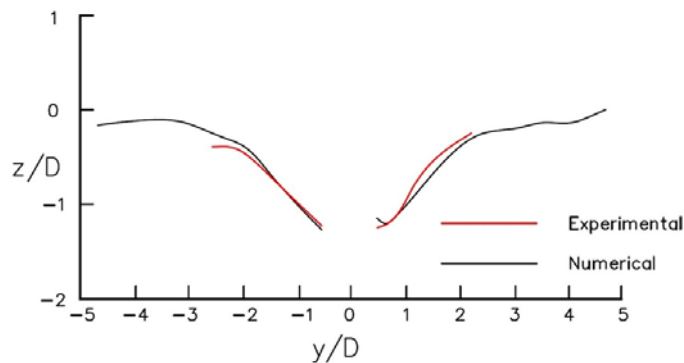


Fig. 6: Scour depth distribution along y-axis. (For $h_c/D=2.5$).

10. Comparing Scour Depths in Numerical and Physical Models:

Fig. (7),(8) compares the scour depths in physical and numerical models. The variations of scour depths showed goods agreement with the results of the physical model as such the calculated S/D for $h_c/D=2.5$ is almost 20% lower and for $h_c/D= 0.25$ is almost 10% lower than experimental results, respectively. Reviewing Fig. (7),(8) shows that at the earlier stages of scour, depth variations are more evident while they decrease in time until scour depth becomes constant.

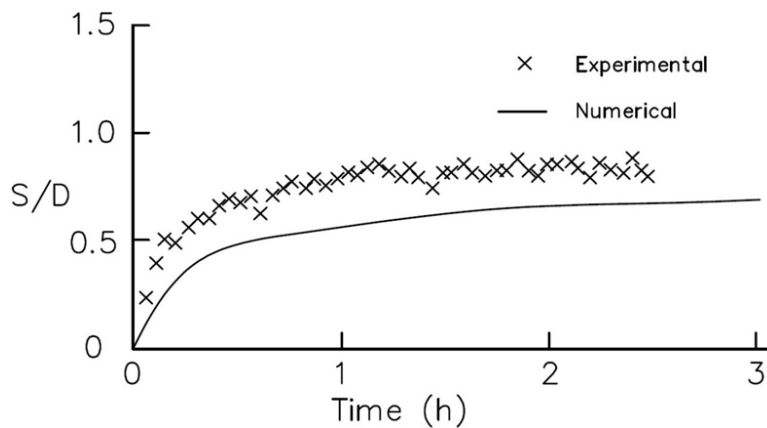


Fig. 7: Simulated and measured scour depth development at the front edge of the cylinder. (For $h_c/D=0.5$).

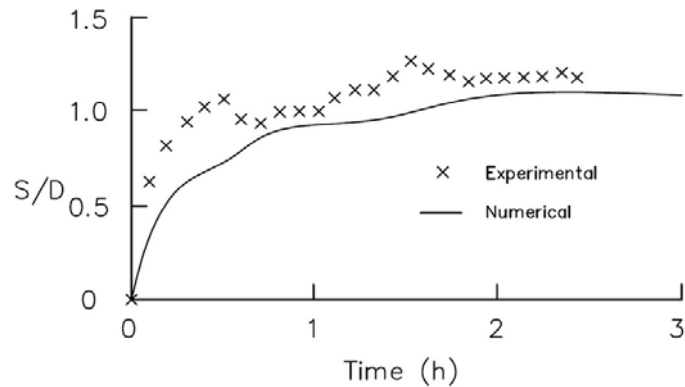


Fig. 8: Simulated and measured scour depth development at the front edge of the cylinder. (For $h_c/D=2.5$).

11. Comparing Scour Depths in Numerical and Experimental Models for Surrounding Area of Bridge Pile:

Fig. (9),(10) shows the comparisons of scour depths at surrounding area of bridge pile. As it is observed, maximum scour depth occurs at point and is reduced as flow moves downstream. Also shows the calculated scour depths by numerical model at surrounding area of bridge pile is 8% larger than that calculated by experimental model.

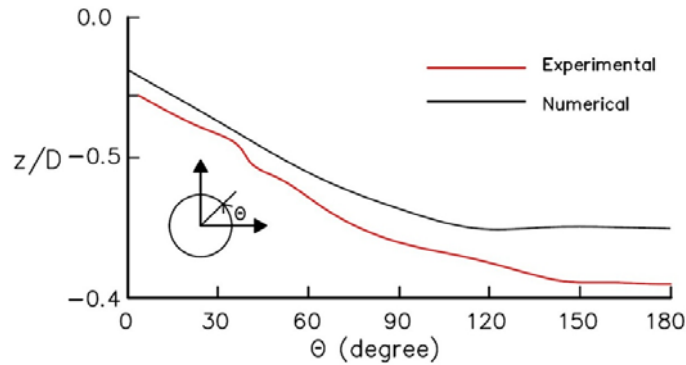


Fig. 9: Scour depth distribution along cylinder surface. (For $h_c/D=0.5$).

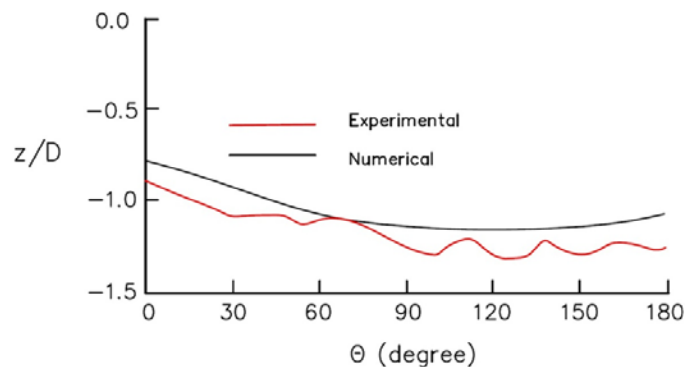


Fig. 10: Scour depth distribution along cylinder surface. (For $h_c/D=2.5$).

Conclusions:

The results indicate that SSIIM model is capable of three-dimensional simulation of flow and sediment around a bridge pile with high accuracy and it considers the effects of downward flows in front of pile and horse-shoe vortices around pile in determining bed stage variations. Also, it takes into account wave front of a pile and calculates water profile. This model proved dependable for similar applications. Scour mechanism due to horse-shoe vortices and vortex release phenomenon were properly simulated by model.

The predicted scour depth by existing models is measured 10 to 20% smaller than that by experimental models.

Reduction of bridge pile height weakens the effects of horse-shoe vortex and vortex release phenomenon. It was also observed that should the bridge pile height be reduced, scour depth should also be reduced. The scour depth variations have an exponential relation with bridge pile height reduction. When height-to-diameter ratio of bridge pile exceeds 2, scour depth acts independently from h_c value.

Scouring process is determined by the combination of horse-shoe vortex and vortex release phenomenon. Sediments near upstream flow surface are washed away through horse-shoe vortex and turned into suspended particle and then transported downstream. The scoured materials cause bed slope in front of bridge pile and sedimentation on front edges of scour basin towards bridge pile.

It was observed that scoured bed slope in front of bridge pile was always too close to sedimentation stagnation angle. horse-shoe vortex plays a significant role in scouring process on bridge pile bed. When bridge pile is small enough ($h_c/D < 0.5$), no scouring is observed on bridge pile bed due to vortex release phenomenon. The investigations on effective factors of scour phenomenon showed that the increase of flow speed, discharge of inflow to channel, upstream flow depth [as a hydraulic parameter] and bridge pile diameter may result in the increase of scour depth around bridge piles.

REFERENCES

- Ansari, A. and A. Qadar, 1994. Ultimate Depth of Scour around Bridge Piers, New York: Of National Hydraulics, Conference.
- Breusers, H., G. Nicollet and H. Shen, 1977. Local Scour around Cylindrical Piers, *Iahr: Journal of Hydraulic, Research*.
- Brooks, H.N., 1936. discussion of .Boundary shear stresses in curved trapezoidal channels., by A.T.
- Chang, W., J. Lai and C. Yen, 1999. Simulation of Scour Depth Evolution at Pier Nose, Proceedings of the 1999 International Water Resources Engineering Conference, August, Session BS-05, Water Resources Publications, LLC, Highlands Ranch CO.
- Chiew, Y., 1992. Scour Protection at bridge Piers., *Journal of Hydraulic Engineering*, 118(11): 1260-1269.
- Ettema, R., 1980. Influence of Bed Material Gradation on Local Scour, New Zealand: The University of Auckland.
- Kumar, V., 1996. Reduction of scour around bridge piers using protection devices, Indian: University of Roorkee.
- Kumar, V., K. RangaRaju, and N. Vittal, 1999. Reduction of local scour around bridge piers using slot and collars, *Journal of Hydraulic Engineering*, 125(12): 1302-1305.
- Laursen, E., 1966. Scour around Bridge Piers and Abutments, Iowa: Iowa Highway Research, Board.
- Md.Faruque, Mia., Hiroshi Nago, 2003. " Design Method of Time – Dependent Local Scour at Circular ridge Pier" *J. of Hydr. Eng, ASCE.*, 129(6).
- Melville, B. and S. Coleman, 2002. Beidge Scour, Colorado: Water Resources Publications, LIC, Colorado.
- Mueller, D. and R. Chad, 2002. Analysis of pier scourpredictiona and realtim field measurements, Texas: Texas A and M Uuiversity.
- Niemann, H. and N. Holscher, 1990. A review of recent experiments on the flow past circular cylinders, *Aerodyn*.
- Olsen, B., 2003. SSIIM Manual, www.bygg.bygg.ntnu.
- Olsen, B., 1999. Computational Fluid Dynamics in Hydraulic and Sedimentation engineering, www.bygg.ntnu.
- Olsen, N.R.B., 2007. "SSIIM Users' Manual", The Norwegian University of Science and Technology. 21.
- Schlichting, H., 1979. "Boundary layer theory", McGraw-Hill.
- Olsen, B., 2001. CFD Modeling For Hydraulic structures, www.bygg.Ntnu.
- Olsen, B., 1999. Kjelesvig, M., Tree Dimentional Numerical Flow Modeling For Estimation of Maximum Local Scour Depth, *J. Hydr., Eng.*
- Van Rijn, L.C., 1987. "Mathematical modeling of morphological processes in the case of suspended sediment transport", Ph.D thesis, Delft University of Technology.
- Zaredehdasht, E., H. Hassunizadeh, M. Mahmoodian Shooshtari, M. Akbari, M. Ghasempour, 2010. An examination of the water erosion incursion in too the bridge pillars through the method of slipping the pillars using the numerical model of data analysis of FLUENT, *Australian journal of basic and applied science*, Pakistan. No. 3274.